STM JOURNALS

Journal of
Polymer & Composites

ISSN: 2321-2810 (Online)
ISSN: 2321-8525 (Print)
Volume 13, Special Issue 1, 2025
DOI (Journal): 10.37591/JoPC

https://journals.stmjournals.com/jopc

Research JoPC

Quantification of Snow/Glacier Melt Impacts of Historical and Future Climate Change on Eastern Himalayan River

A K Shukla [1],*, I Ahmad [2], S K Jain [3], M K Verma [4]

Abstract

Millions of the population on Eastern Himalayan Rivers (EHR) totally depend on, domestic use, agriculture, and hydropower. Several studies found that climate warming threatens this EHR's hydrological regime. In order to understand the hydrologic response of their headwaters and how climate change affects streamflow, a hydrological modeling study is conducted in the Teesta River Basin (TRB) in EHR using an open-source Quantum Geographical Information System (QGIS) with semi-distributed QSWAT1.5 (Soil and Water Assessment Tools). The model performed well in 1985-2015 simulations, warmup period (2001-2002) for calibration (2003-2010) and validation (2011-2015) versus measured daily streamflow at Teesta IV DAM (R2 ≈ 0.87). The study found that snowmelt runoff from a bigger snow-covered area at higher TRB accounts for 62–74% of the average annual water supply of 2000 mm on average 200. Approximately 16% of precipitation is evapotranspiration. Basin water yield is 78% of precipitation, with most generated in early summer from mid-May to September. The Coupled Model Intercomparison Project Phase 6 (CMIP6) data for thirteen models, which ACCESS-ESM1-5 was the most suitable model, which was calculated by the Taylor diagram. CMIP6 has four Shared Socioeconomic Pathway scenarios (SSPs), but the research has used average data to explore how climate change will affect future streamflow. First, calculate monthly discharge for all SSPs but got the same result from all, and model performed well. Global Climate Models (GCM) to Regional Scale Model (RCM) and Quantile Mapping are used to correct bias and load into SWAT to simulate end-of-century stream flows. The region's predicted precipitation and temperature fluctuations showed a wetter and warmer climate.

Keywords: TRB, snowmelt, QGIS, runoff, CMIP6 & SWAT

***Author for Correspondence**
A K Shukla

[1] Research Scholar, Department of Civil Engineering, NIT Raipur, GE Road, Chhattisgarh, India
[2]Assistant Professor, Department of Civil Engineering, NIT Raipur, GE Road, Chhattisgarh, India
[3]Visiting Professor, Department of Civil Engineering COEDMM, IIT Roorkee, Haridwar Road, Uttarakhand, India
[4]Assistant Professor, Department of Civil Engineering, NIT Raipur, GE Road, Chhattisgarh, India

Received Date: April 23, 2024
Accepted Date: June 19, 2024
Published Date: December 18, 2024

Citation: A K Shukla, I Ahmad, S K Jain, M K Verma. Quantification of Snow/Glacier Melt Impacts of Historical and Future Climate Change on Eastern Himalayan River. Journal of Polymer & Composites. 2025; 13(Special Issue 1): S508–S524p.

INTRODUCTION

The Indian Himalayas are facing an increasingly dangerous situation due to the rapid loss of snow and glacier mass, which poses a significant risk to the region's ecological importance and awe-inspiring nature [6&9]. This tendency has experienced a rapid increase in the past several years. The towering peaks in question are commonly known as the "Water Towers of Asia" because to their role as the source of several significant rivers, including the Ganges, the Brahmaputra, and the Indus. These rivers provide water to millions of people throughout South Asia [25 & 24]. The snow and glacier cover in the Indian Himalayan region is experiencing significant depletion due to the direct impact of increasing global temperatures, which is attributed to climate change. The melting of glaciers caused by this trend has a substantial influence on water resources. It has the potential to decrease the available water, change the patterns of hydrological flow, and raise the probability of glacial lake outburst floods (GLOFs) [15]. Furthermore, the downstream communities that depend on this water for agricultural activities, drinking water, and the generation of hydropower are at risk [32].

James Hansen, a well-known climate scientist, made the observation that "our planet has become a snowball, and the snowball is picking up speed as it rolls downhill." The current state of affairs in the Indian Himalayas demonstrates how important it is to take immediate action to combat the effects of climate change and put adaptation strategies into place. These activities could include better water resource management, monitoring glacier health, and adopting sustainable farming and land-use practices. It is a harsh reminder of the global climate crisis and the critical need to safeguard this vital resource for the benefit of both the local populations and the broader ecological stability of the region as the glaciers in the Indian Himalayas continue to recede. This is because protecting this resource is beneficial to both the local community and the broader ecological stability of the region.

The Brahmaputra river basin is situated in the north-eastern region of the Indian subcontinent and forms a valuable geographical and ecological asset of great importance [11 & 28]. This river system has played a crucial role in the social, economic, environmental, and cultural welfare of the region for ages. The Brahmaputra River, which has its source in Tibet and is referred to as the "YarlungTsangpo," follows a winding course through India and Bangladesh before finally discharging into the Bay of Bengal [14]. The ecological significance of these river basins cannot be overstated. Their distinct ecosystems support a wide variety of plant and animal life, with species that have evolved to thrive in the region's particular climate and topography [36-37]. Furthermore, the rivers play a crucial role in sustaining a prosperous fishery industry that is essential for the local economies. Given the presence of climate change and the growing impact of human activities, it is imperative to acknowledge the vulnerability of these ecosystems [14 & 20]. In this regard, the words of the respected environmentalist and novelist Aldo Leopold hold great significance. He states, "Conservation is the establishment of a harmonious relationship between humans and the land." The maintenance of a harmonious equilibrium between human progress and ecological conservation in the Brahmaputra and Teesta river basins is crucial for the long-term preservation of the region's scenic splendour, diverse array of species, as well as the sustenance and welfare of the communities reliant on these water resources [1]. This first feeling succinctly captures the pressing need and significance of responsible administration, safeguarding, and environmental protection endeavours in these critical river basins.

The TRB has experienced notable modifications in precipitation patterns and temperatures due to climate change, resulting in important consequences for the hydrology, agriculture, and ecosystems of the region [27]. In recent years, an increasing amount of precipitation and temperature i.e. scientific study has shown solid proof of these shifts. Research has shown a significant rise in temperature, with average temperatures increasing, along with a modified pattern of rainfall distribution throughout the year [8]. The fluctuating temperature patterns possess the capacity to impact the nearby microclimate, hence influencing the growth of crops and the availability of water. This is of utmost importance for the sustenance of communities residing in the basin [16 & 29,30]. Furthermore, the modified precipitation patterns, characterized by a growing frequency of heavy rainfall occurrences, have resulted in an elevated susceptibility to floods and landslides in the area. These severe climatic phenomena can disturb routine activities, harm the physical structures, and pose a risk to the well-being of the inhabitants residing in the TRB [31]. These climatic changes are frequently linked to global climate change and have led regional governments and international organizations to adopt measures for adaptation and resilience. According to Nobel laureate Al Gore, the climate catastrophe is not merely a political matter but rather a moral and spiritual test that affects all of humanity. Furthermore, it presents a significant chance for us to elevate worldwide awareness to a more advanced state. The Teesta River watershed exemplifies how climate change surpasses national borders and requires a united ethical and practical reaction. Adapting to the evolving climate conditions in the Teesta basin is not solely an issue of ecological conservation but also a moral obligation to safeguard the welfare and livelihoods of the communities residing in this crucial area.

The SWAT model is an esteemed and extensively employed technique in the realm of hydrology and watershed management, particularly for evaluating glacier and snowmelt runoff in mountainous areas [32]. This model offers a sturdy framework for replicating the intricate processes that take place in these places, making it especially pertinent in areas that largely rely on the seasonal storage and discharge of water from glaciers and snowpack [36]. The SWAT model has the ability to simulate a range of land surface processes, including snow built-up and melting, evapotranspiration, infiltration, and the formation of runoff [33]. It considers the unique geographical and meteorological characteristics of mountainous areas. The model takes into account variables such as temperature, precipitation, topography, and land use to predict when and how much glacier and snowmelt runoff will flow into river systems [38]. It is essential to comprehend and control water resources in areas where this discharge plays a substantial role in the whole water supply. Due to the escalating effects of climate change, mountainous regions are experiencing a rapid decline in glacier size, posing significant implications for the supply of water downstream [38]. The SWAT model is a valuable tool for forecasting and managing the effects of glacier melt and snowmelt on local hydrology and water resource availability [12 & 22]. It enables researchers and policymakers to evaluate the repercussions of these changes. The model coincides with the statement made by David Suzuki, a renowned environmentalist that "Water and air, the fundamental fluids crucial for all forms of life, have transformed into worldwide repositories for waste." Utilizing the SWAT model for analyzing glacier and snowmelt runoff is crucial for effectively managing these rich water resources in a changing climate, with a focus on sustainability and responsibility [38].

When it comes to hydrological modeling, particularly in the context of snowmelt runoff forecasting, the Sufi2 algorithm is an advanced and cutting-edge piece of software that plays a critical role as a key component [13, 18 & 33]. It uses cutting-edge optimization strategies to boost the realism of hydrological models and hone its capacity to predict snowmelt processes. In this context, the Nash-Sutcliffe Efficiency (NSE), and the Coefficient of Determination (R^2) are two objective functions that are frequently applied. The goodness-of-fit between observed and simulated values is measured using the NSE, and R^2 is a quantification of the proportion of the variance in the observed data that is explained by the model, which provides insights into the model's explanatory power [2 & 17]. R^2 measures the proportion of the variance in the observed data that is explained by the model. Researchers are able to improve their snowmelt modeling efforts by optimizing these objective functions with the Sufi2 algorithm.

R, a computer language widely used in data analysis and modeling, is highly robust and adaptable, making it ideal for analyzing snowmelt. Researchers often employ R [21, 32 & 35] to construct, refine, and evaluate hydrological models for snowmelt processes. The Taylor diagram is a valuable tool in this context as it allows for the assessment of a model's performance by visually comparing many model output metrics with observations [7, 10& 26]. The Taylor diagram provides a comprehensive view of the goodness-of-fit, specifically emphasizing the correlation coefficient (R), root mean square error (RMSE), and standard deviation ratio. Researchers can use this opportunity to assess the most appropriate model for analyzing snowmelt by considering both the model's accuracy and its ability to reflect observed variability. The combination of R programming and the Taylor diagram has shown to be a valuable tool in enhancing our understanding of snowmelt dynamics and boosting our capacity to manage water resources in snow-dominated regions.

Study Area

The TRB is a significant Brahmaputra River tributary and adjoined with nine major tributaries in the upper Teesta to lower Teesta basin. EHR that lies within the boundaries of Nepal and Bhutan and covers the entire state of Sikkim. For the purposes of this study, the upper portion of the Teesta basin, all the way up to the Teesta IV Dam, has been chosen to obtain the historical and projected future stream flow. As can be seen in Figure 1, the basin covers an overall size of approximately 8141.59 km^2 and extends geographically between the coordinates of 27°04'52" and 28°08'26" North Latitude and 88°00'57" and 88°55'50" East Longitude. The ChhomboChhu and KhangchungChho glacier lakes are the primary sources of the Teesta River. These lakes are located in the northeastern corner of Sikkim at the height of 5281 meters [3]. The elevation of the basin ranges from 800 to 6048 meters. The ZemuChhu, the LachungChhu, the RangyongChhu, the DikChhu, the Rani Khola, the RangpoChhu, and the RangitRiver are all important tributaries [4, 5 & 23].

The majority of the basin that is glaciated may be found in the northern half of the Eastern Himalayas [34]. This region of the Himalayas is home to a wide range of plant and animal species. It is home to more than 400 lakes formed by glaciers. The majority of these can be found at an altitude of more than 4500 metres. According to the Census from 2011, the mean annual rainfall ranges between 2,000 to 4,000 millimetres due to altitude. The Teesta River receives the majority of its water from precipitation and melted snow, according to research done by SC Mukhopadhyay in 1982 and Tsering et al. in 2019 respectively. The temperature ranges from 1.5 degrees Celsius to 9.5 degrees Celsius at a lower altitude, with the highest temperature being recorded in the months of July and August (21 degrees Celsius to 26 degrees Celsius), and the lowest temperature being recorded in the months of December and January (between 6 degrees Celsius and 8 degrees Celsius) (Census, 2011). According to research done by Jain et al. in 1998, the primary source of water for the Teesta river during the spring season is the snowmelt runoff from the higher altitudes in the eastern Himalayas.

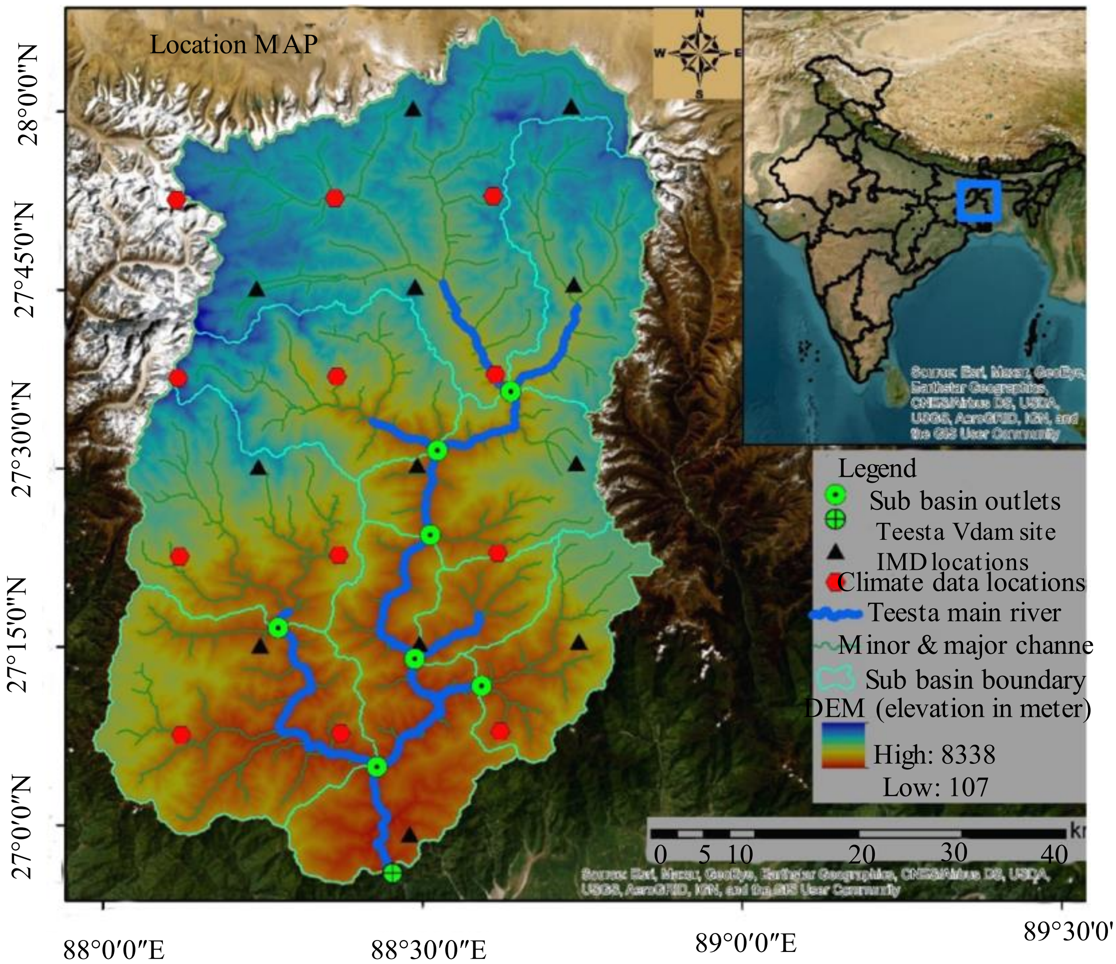

Figure 1. Location map of Teesta river basin.

Data Used

The hydrologic response of the Satluj river basin was modelled with the help of several maps that were created using geospatial data. The catchment area was determined with the help of DEM (Digital Elevation Model) ALOS Palsar Hi-Resolution Terrain Data that was acquired from Alaska at a resolution of 12.5 metres. The Landsat satellite imagery taken during the month of September in 2003 was used to create the Land Use Land Cover (LULC) map. This imagery contained seven different spectral bands. The Food and Agriculture Organisation (FAO) provided the soil map, which was then georeferenced and transformed using the Universal Transformation Metre (UTM) (Table 1). At a resolution of 30 metres, each and every piece of spatial data was analysed. On the basis of LULC that was derived from satellite imagery, the major classes of LULC are different from upper to lower Teesta. This can be seen moving down the mountain. Snow and ice account for 24.47% of the total land area, whereas forest cover accounts for roughly 43%, and uncultivated land accounts for 9.61%. In terms of the soils, the glacier area accounts for 14.37% of the total, while moraines and loamy soils make up the balance of the predominant types in the region.

The information pertaining to the weather is broken up into two categories: primary and secondary. The primary source's precipitation (PRCP), as well as its minimum and maximum temperatures (TMPR), are recorded here (Fig 2 & 3). The supplementary datasets consist of the relative humidity (RHMD), wind speed (WIND), and solar radiation (SLRD) measurements. Downloads were taken from two different places for each day's worth of meteorological information covering the research area from 1985 to 2015. The Indian Meteorological department (IMD), located in India, is where PRCP and TMPR are downloaded from. The data for RHMD, WIND, and SLRD were all downloaded for the same time period from the official website of Power NASA. The daily future CMIP6 data from https://zenodo.org link [19] (Table no. 2). It was Bias Corrected Climate Projections from CMIP6 Models for South Asia and the spatial resolution was 0.25 including PRCP and TMPR. The study region contains a total of 12 stations, all of which were created in SWAT format. The National Institute of Hydrology (NIH), Headquarter Roorkee, India, in order to acquire the daily discharge outflow data from 2003 to 2014 at the mouth of the basin, which was measured by the Teesta IV DAM gauging station. These data were utilised for the objectives of model calibration as well as validation. Future climate change will have on streamflow beginning in the year 2016 and continuing until the year 2099 which was equally divided i.e. 28 years in Near Future (NF from 2016-2041), Middle Future (MF from 2042-2071) and Far Future (FF from 2072-2099).

METHODOLOGIES

SWAT Model Description

The SWAT is a versatile hydrological modeling model that was made by TAMU (Table no. 3). The model is physically based and semi-distributed, taking input as the hydrological cycle, land use, soil characteristics, and weather data. Hydrological response at the basin outlets in the form of runoff, groundwater flow, sediment transfer, and the movement of nutrients and pesticides (see in figure 4). It is a useful tool for watershed management and environmental impact studies because it can be used to look at how different land management scenarios, changes in land use, and conservation practices affect the amount and quality of water. In order to show how things change over space in the models, the catchment area is split into sub-catchments, which are then split into hydrologic response units (HRUs). An HRU has been created by the use of unique class features, i.e., types of slopes, Classification of LULC, and types of soils in the basin. Before the preparation of the HRUs model, it was given the notification of excluding features because some parts of the basin had very little area, and also, each sub-basin was split into ten elevation bands based on the percentage slope [21].

The model figures out how much snow melts and evaporates in each elevation band, and then it figures out the weighted average for each sub-basin. SWAT uses a temperature-index method. It does this by controlling the effect of the previous day's temperature on the current day's temperature. SWAT uses an exponential function of soil depth and water content to determine how much water evaporates from the earth. The changed SCS-CN (Soil Conservation Service-curve number) method was used to figure out flow by looking at how the land was used, the type of soil, and the amount of water present. There are different layers of soil that help water move through the soil and do things like evaporate, be taken up by plants, run laterally, infiltrate, and percolate to lower layers. Since the model keeps a constant water balance, the subdivision of the area lets it show how evapotranspiration varies for different crops and soils. The runoff from each sub-basin is generated separately, and the total runoff from the basin is found by going through the paths of all the runoff from each sub-basin. It gives a more accurate picture of the water balance and makes the data more reliable. For more information, the reader is told to look at previous works that have written a lot about the model.

Table 1. Satellite and Data layer description.

S N.	Data Layer/Satellite name	Resolution (m)/Band (combination)	Year/Period	Sources
1	DEM/AlosPALSAR	12.5/FBS	2011/Single	https://asf.alaska.edu/
2.	LULC/Decadal Data & SWAT-TAMU		2005/Multiple	https://daac.ornl.govhttps://swat.tamu.edu/
3.	LULC/Landsat	30.0/FCC	2005/Single	https://earthexplorer.usgs.gov/
4.	Soil/FAO	250/Image		https://www.fao.org/soils-portal/en/
5.	Whether Data/IMD & Power NASA	Vary from 0.25-1º/all Data	1985-2014	https://cdsp.imdpune.gov.in/
6.	Climate Data/CMIP6	0.25º	2016-2099	https://zenodo.org/records/3987736
7.	Discharge Site/Teesta IV DAM	Single Site	2003-2014	National Institute of Hydrology, Headquarter, Roorkee

Table 2. Description of CMIP6 Model.

S N.	Model Name	Institute Name	Country	Resolution (LAT*LONG)
1	ACCESS-CM2	Commonwealth Scientific and Industrial Research	Australia	he
2	ACCESS-ESM1-5	Organization and Bureau of Meteorology	Australia	
3	BCC-CSM2-MR	Beijing Climate Center, China Meteorological Administration	China	1.12*1.12
4	CanESM5	Canadian Centre for Climate Modelling and Analysis	Canada	2.79*2.81
5	EC-Earth3	EC-EARTH consortium	Europe	0.70*0.70
6	EC-earth3-Veg	EC-EARTH consortium	Europe	
7	INM-CM4-8	Institute for Numerical Mathematics	Russia	1.50*2.00
8	INM-CM5-0	Institute for Numerical Mathematics	Russia	
9	MPI-ESM1-2-HR	Max Planck Institute for Meteorology	Germany	0.94*0.94
10	MPI-ESM1-2-LR	Max Planck Institute for Meteorology	Germany	1.87*1.88
11	MRI-ESM2-0	Meteorological Research Institute	Japan	1.12*1.13
12	NorESM2-LM	Norwegian Earth System Model	Norway	1.89*2.50
13	NorESM2-MM	Norwegian Earth System Model	Norway	0.94*1.25

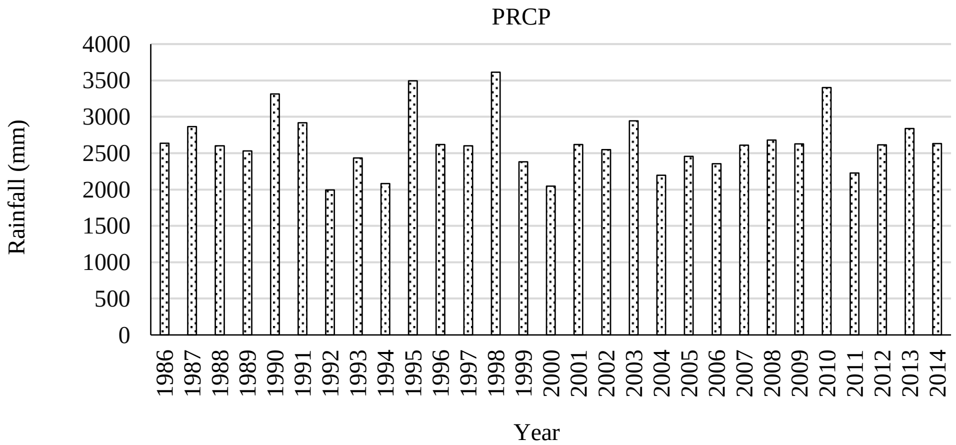

Figure 2. Rainfall graph of Teesta river basin.

Journal of Polymer & Composites
Volume 13, Special Issue 1
ISSN: 2321-2810 (Online), ISSN: 2321-8525 (Print)

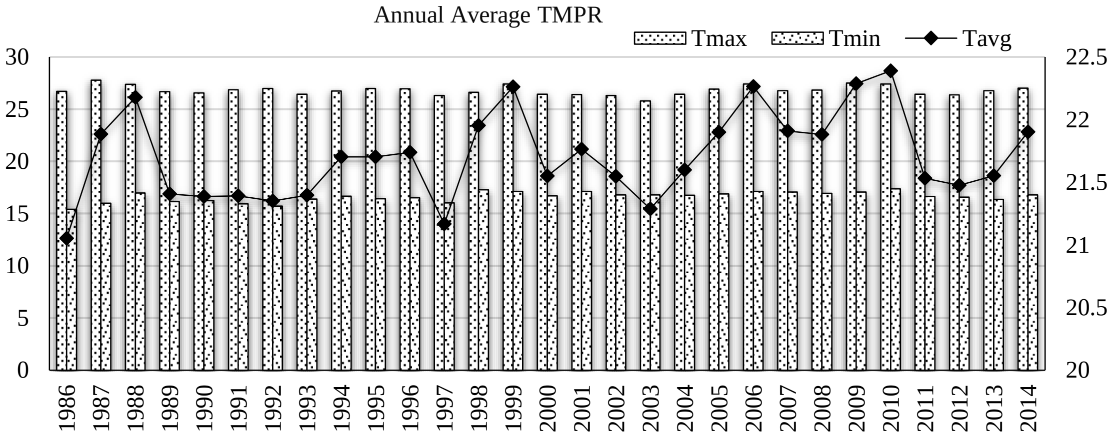

Figure 3. IMD annual average temperature of Teesta river basin.

Table 3. Software data and sources.

S.N.	Software & Plugin Description	Sources
1	QGIS 3.16 (Hannover)	https://qgis.org/en/site/
2	QSWAT3 1.5.2	https://swat.tamu.edu/
3	SWATCUP	https://swat.tamu.edu/
4	R-Studio	https://posit.co/
5	Microsoft Office	https://www.office.com/

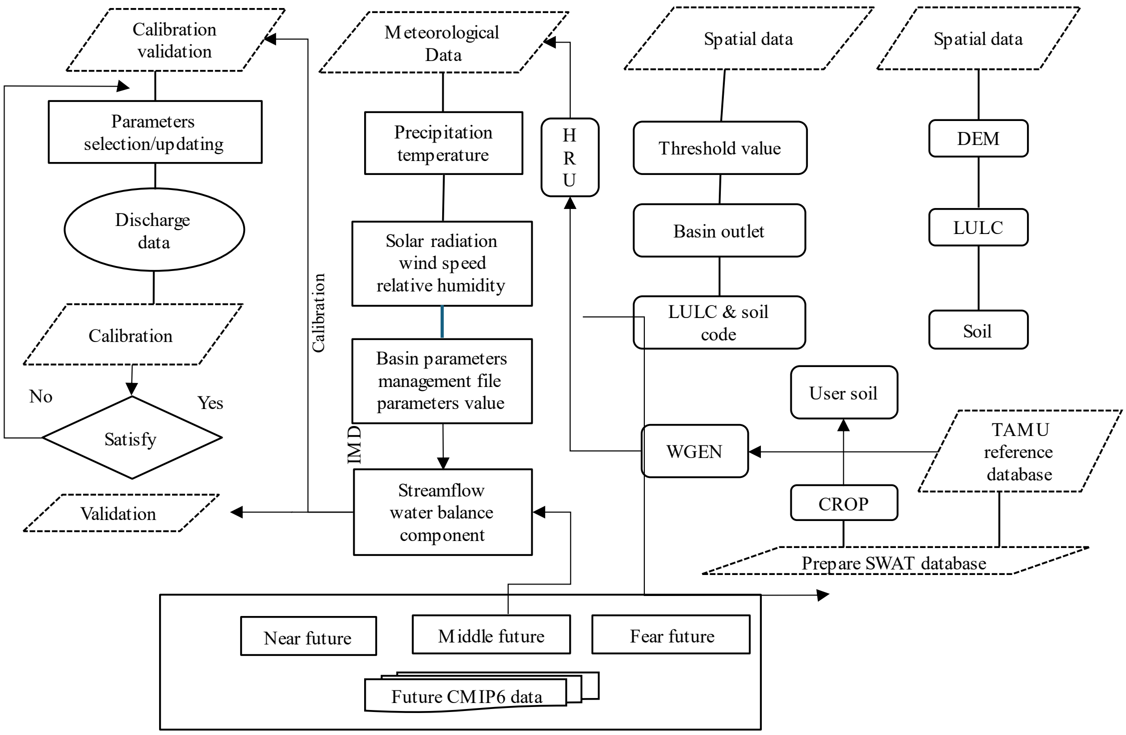

Figure 4. Adopted methodologies.

Data Preparation for Model Setup

In order to effectively simulate and analyze the complex hydrological processes that occur within a specific watershed, the SWAT model is dependent on the comprehensive integration of spatial and non-spatial variables, Climate, and the SWAT2012 database. The geographical datasets, which include DEM, LULC, and Soil information, are of exceptional significance because they define the physical characteristics of the watershed and exercise control over hydrological processes, water flow, sediment transport, and pollutant movement. This gives the spatial datasets a special place in the hierarchy of importance. The model's capability to effectively replicate watershed dynamics is directly impacted by the quality, resolution, and precision of the spatial datasets used in the modeling process. These datasets include a wide variety of physiographic and topographic variables, whereas the LULC data is generated through the application of supervised classification techniques with reference to decadal LULC data. Despite having different geographical resolutions and projections, all datasets are harmonized into the same grid format to simplify compatibility and integration. This ensures that there is an overlap that is greater than 95%. Notably, high-resolution DEM data is modified, with a grid size of 30x30 meters and UTM 45 Zone projection. At the same time, LULC and Soil datasets go through re-projection and grid size to align with the standardized format. Non-spatial datasets, like the supporting files for LULC and soil type, include vital information on LULC and soil types, and they recall this information/unique code throughout the processing stage. In addition, Climate Data includes time-series data relating to important climate variables, such as PCRP, TMPR, WIND, SLRD, and RHMD, as well as observed streamflow data from discharge gauge sites or the major outlet points of each sub-basin.

For the SWAT model to effectively describe the spatiotemporal variability of hydrological processes throughout the watershed, it is essential to use both spatial and non-spatial datasets in an integrated manner. In order to make effective use of SWAT for understanding and managing water resources, evaluating the impacts of changes in land use, and addressing the challenges posed by climate change in a manner that is scientifically rigorous, proper data management, pre-processing, and calibration procedures are indispensable scientific steps. The development of the SWAT2012 Database was prepared by utilizing the example datasets given by itself the model crop patterns and soil types are furthermore important for hydrological modeling and watershed management because all characteristics play a major role in the processing. For the WGEN file the GUI-based MS ACCESS application with the help of all daily time series data & and station files along with geographical coordinates and elevation. For that data was taken from the SWAT-TAMU website and some relevant literature.

Correlation Between IMD & CMIP6

The application of R programming techniques in assessing the correlation between the IMD and the CMIP6 through tools like the Taylor diagram. Taylor diagrams summarize relationships between patterns based on correlation, root-mean-square difference, and variance ratio. The Taylor diagram lets you compare variables from multiple models or reanalyses to reference data. Observational data (reanalysis) or another model or control run can be used as reference data. This may require re-gridding because all variables must be on the same grid. It is of significant scientific importance. IMD, a total of 12 stations covering the entire watershed. It collects extensive observational data to provide weather forecasts and monitor climate patterns in the region. In contrast, CMIP6 offers a climate/future of data generated by complex climate models, enabling global-scale climate projections. Machine learning methods can serve as a vital intermediary, helping to unravel the relationships and correlations between these disparate datasets. As a visual tool, the Taylor diagram facilitates the comparison of statistical measures such as correlation coefficients, root mean square error, and standard deviations, providing a comprehensive view of the agreement between IMD's observations and CMIP6 model outputs.

Taylor Diagram

The purpose of a Taylor diagram is to show visually which of several possible models or representations of a system, process, or event is the most accurate. This diagram, created by Karl E. Taylor in 1994 and released in 2001, makes it easier to compare different models. Three statistics measure how well the modelled behaviour matches up with what was observed: the standard deviation, the root-mean-square error (RMSE), and the Pearson correlation coefficient (see in Figure 5).

Taylor diagrams have mostly been used to test models that try to study climate and other parts of Earth's environment, but they can also be used for things that aren't related to environmental science, like showing how well fusion energy models match reality. Many types of tools, both free and paid, can be used to make Taylor diagrams. These include GrADS, IDL, MATLAB, NCL, Python, R, and CDAT. As a conclusion, a Taylor diagram offers a condensed method for evaluating the performance of a model in a number of different dimensions, such as the variance, the correlation, and the general agreement with the data that has been seen. Through the use of the visual representation, researchers and modellers are able to immediately determine the strengths and flaws of model simulations. A well-performing model will be closer to the reference point, with a smaller distance from the origin and a smaller angle with regard to the azimuthal axis. In addition, the model will have a smaller angle.

Uncertainty and Calibration & Validation using R-Programming

First, download the R and R studio because this GUI-based tool runs only specific versions and is based on a window-based program. After that, install the R package known as shiny. It was installed by simple string, i.e.,install.packages ("shiny"). Utilizing R-Programming inside the SWAT-CUP (SWAT Calibration and Uncertainty Programs) framework is one way to improve the resilience of hydrological modeling processes, including uncertainty quantification, calibration, and validation. These components are fundamental components of hydrological modeling. The Soil and Water Assessment Tool, also known as SWAT, is a complicated hydrological model, and SWAT-CUP is a flexible tool that is used to calibrate SWAT. Researchers now have access to a wide variety of statistical and machine-learning approaches, which makes it easier for them to do uncertainty analysis, calibration, and validation of SWAT model parameters. This is made possible thanks to the integration of R-Programming. When dealing with complicated and linked hydrological processes, it is especially important to characterize the uncertainty associated with the model inputs and parameters, which can be accomplished with the help of these strategies (Table no. 4). During the calibration phase, SWAT-CUP's utilization of R-Programming makes optimizing the model's parameters possible, enabling the model to be fine-tuned to correspond with observed data. After that, the model's performance may be thoroughly verified against different datasets simultaneously. This combination of SWAT-CUP and R-Programming speeds the uncertainty management process and parameter calibration in SWAT, eventually leading to more accurate hydrological modeling results. Accurate hydrological modeling results are an essential component of efficient water resource management and assessment of the impact of human activities on the environment.

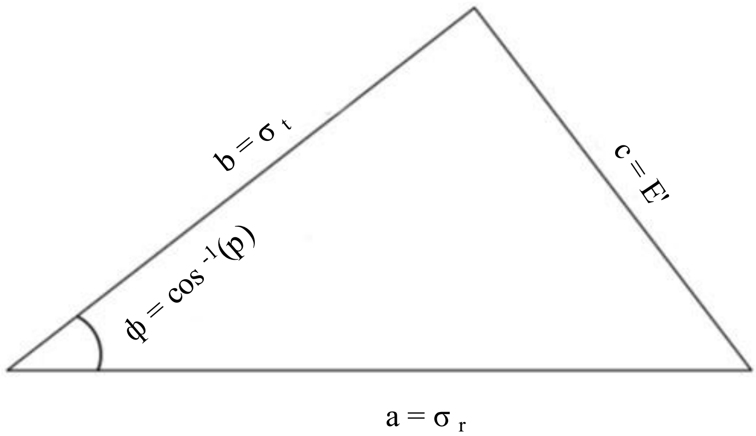

Figure 5. Diagram for taylor diagram.

Table 4. Range of objective function

S.N.	Objective functions	Range	Satisfactory value	Average/good	Best
1.	R2	0 to 1	>0.5	0.5≤R2≤0.75	0.75<R2≤1
2.	NSE	-∞ to 1	>0.5	0.5≤R2≤0.75	0.75<R2≤1
3.	MNSE	-∞ to 1	>0.5	0.5≤R2≤0.75	0.75<R2≤1

RESULTS

Model reliability is based on calibration and validation results. The most sensitive parameters were identified and ranked by their impact on expected outcomes using sensitivity analysis. The model parameters were methodically updated during calibration to produce the most accurate results compared to the data. The stable calibration parameters were used to model the catchment response during validation. The experimental and simulated hydrographs were compared to evaluate the model. The simulation results were analysed using three statistical criteria, including the R2 value. The model performed well when R2 and NSE were close. Calibration data length is crucial to modelling. Most accessible data was separated into calibration and validation periods. According to Yapo and colleagues' 1996 study, a model that is somewhat insensitive to the period chosen must be calibrated with data from at least eight years. Thus, 1986–2014 is the simulation era in this study. However, 2003–2010 and 2011–2014 are used to calibrate and validate the model. The initial three-year data period, from 1986 to 1989, is called the "warm-up" period to reduce simulation errors caused by incorrect starting conditions. This is done by using TRB daily streamflow data from the Teesta IV dam gauging station from 2003 to 2014 (Figure 6).

SUFI2 aims to bracket most measured data with the lowest uncertainty band. To measure the power of a calibration/uncertainty analysis and specify the termination rules for SUFI2 iterations, consider the percentage of observations bracketed by the 95% prediction uncertainty (95PPU) (P-factor) and the average width of the 95% prediction uncertainty band divided by the observed data's standard deviation (R-factor). The model is effectively calibrated if the P-factor is larger than 50%, the R-factor is minimal (typically less than 1), and more than 50% of the observed data are bracketed inside the uncertainty bound. This study included twenty iterations, increasing the simulation order from five to 100 when parameters were changed. Each of the last twenty iterations had 500 simulations. Parameter sensitivity was determined using multiple regression analysis. The sensitivity analysis considered 22 parameters, nine of which were snowmelt parameters (Table 5). Published SWAT sensitivity assessments informed our analysis. The parameter sensitivity analysis showed that precipitation lapse rate, temperature lapse rate, snowmelt base temperature, snowpack temperature lag factor, and minimum snow melt rate were significantly influential. These factors were less sensitive than catchment-related parameters (Table 5). Table 4 shows the best-fitted ranges and values for additive or multiplicative factors that express uncertainty when linked with an actual parameter value. The daily discharge measured and simulated during the calibration (2003–2010) and validation (2011–2015) periods show that the hydrographs have the same contour. Some high peaks have been underestimated, but others have been replicated well. The lean phase flow is exaggerated and irregular. This may be due to data entry errors or uncertainty like the following: 1) uncertainty about parameters; 2) natural uncertainties, which are caused by natural processes' random temporal and spatial alternation; 3) uncertainty about data; and 4) uncertainty about the model structure, which reflects the model's inability to accurately represent the system. The green 95PPU band on the graphs shows the narrow model output uncertainty.

In the course of the calibration and validation processes, the TRB's water balance components are utilised. There are three primary elements that make up the water balance: the total precipitation that falls on the basin, the actual evapotranspiration that occurs inside the basin, and the water yield, which is the volume of water that contributes to streamflow. The water yield is comprised of three different types of contributions: the contribution from surface runoff, the contribution from groundwater flow, and the contribution from lateral flow to the stream. The findings indicate that the contribution of direct surface runoff to the total amount of water production is significantly lower. There are significant contributions to the water supply that come from both the lateral flow and the groundwater flow. An estimated 23 percent of precipitation is accounted for by ET. The snowmelt provides a considerable contribution to streamflow in the TRB, which accounts for around 68% of the total water production. It has been shown that the water output from the basin accounts for approximately 48 percent of the total precipitation. This figure is derived by adding the contributions of groundwater, lateral runoff, and surface runoff in the streamflow.

Journal of Polymer & Composites
Volume 13, Special Issue 1
ISSN: 2321-2810 (Online), ISSN: 2321-8525 (Print)

Table 5. Description of parameters.

S.N.	Parameter name	Description	Initial
1.	CN2	SCS runoff curve number	35-98
2.	ALPHA_BF	Base flow alpha factor (days)	0-1
3.	GW_DELAY	Groundwater delay (days)	0-500
4.	GWQMN	Threshold depth of water in the shallow aquifer required for return flow to occur (mm)	0-5000
5.	SFTMP	Snowfall temperature	-20-20
6.	SMTMP	Snow melt base temperature	-20-20
7.	SMFMX	Maximum melt rate for snow during year (occurs on summer solstice)	0-20
8.	SMFMN	Minimum melt rate for snow during the year (occurs on winter solstice)	0-20
9.	TIMP	Snowpack temperature lag factor	0-1
10.	SNOCOVMX	Minimum snow water content that corresponds to 100% snow cover	0-500
11.	SNO50COV	Snow water equivalent that corresponds to 50% snow cover	0-1
12.	GW_SPYLD	Specific yield of the shallow aquifer (m3/m3)	0-0.4
13.	PLAPS	Precipitation lapse rate	-1000-1000
14.	TLAPS	Temperature lapse rate	-10-10
15.	SOL_BD	Moist bulk density	0.9-2.5
16.	SOL_AWC	Available water capacity of the soil layer	0-1
17.	SOL_K	Saturated hydraulic conductivity	0-2000
18.	HRU_SLP	Average slope steepness	0-1
19.	CANMX	Maximum canopy storage	0-100
20.	EPCO	Plant uptake compensation factor	0-1
21.	CH_N2	Manning's "n" value for the main channel	-0.01-0.3
22.	CH_K2	Effective hydraulic conductivity in main channel alluvium.	-0.01-500

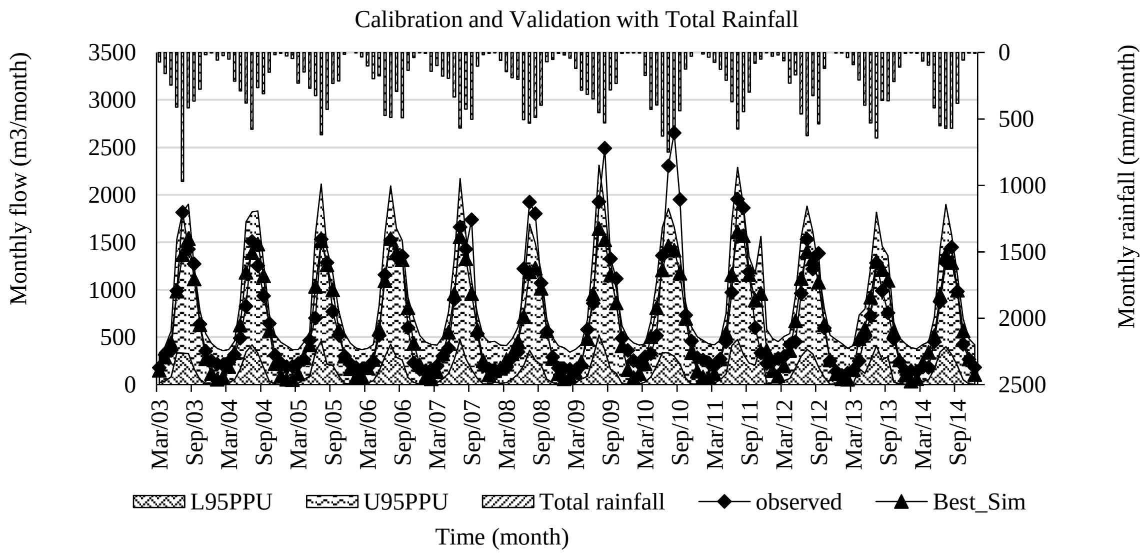

Figure 6. 95PPU Plot with Observed and simulated (Calibration & Validation).

Table 6. Water balance monthly discharge statics with calibration.

Month	PREC	SURQ	LATQ	GWQ	LATE	ET	PET	SEDYIELD	WATERYIELD
JAN	26.67	1.06	8.12	8.54	6.67	10.93	62.36	4.42	20.41
FEB	68.85	24.73	14.15	6.56	12.85	16.15	82.97	133.13	47.38
MAR	130.31	18.57	34.60	11.74	27.74	50.68	135.46	127.25	66.67
APR	148.16	26.90	38.31	18.82	30.68	54.22	113.24	48.64	85.58
MAY	278.12	70.49	68.13	28.25	61.68	71.25	115.30	81.91	168.44
JUN	431.50	134.03	109.98	49.11	112.36	72.35	106.53	117.47	294.96
JUL	596.38	232.76	140.34	84.15	149.08	71.41	110.54	195.47	459.91
AUG	434.88	130.37	122.78	111.00	128.54	55.17	105.87	115.59	367.80
SEP	311.61	80.59	91.90	111.95	94.77	45.97	94.63	119.60	288.60
OCT	134.32	30.92	43.60	98.53	41.76	22.32	89.52	81.58	177.56
NOV	24.74	15.54	5.20	61.84	4.28	1.70	75.60	80.84	86.58
DEC	12.77	0.54	4.02	26.98	4.06	3.89	57.45	2.08	34.96

Table 7. Water balance monthly discharge statics with validation.

Month	PREC	SURQ	LATQ	GWQ	LATE	ET	PET	SEDYIELD	WATERYIELD
JAN	24.47	10.73	6.08	0.10	0.52	7.05	59.80	16.98	34.77
FEB	69.13	37.36	13.78	0.07	1.11	17.20	89.43	51.26	210.12
MAR	97.44	55.44	17.05	0.13	0.80	29.84	136.47	72.67	328.54
APR	173.43	115.58	23.60	0.20	0.78	44.01	103.98	139.40	117.65
MAY	370.20	271.31	41.18	0.39	1.08	55.01	106.88	312.83	194.82
JUN	417.82	316.32	44.11	0.52	1.17	54.74	108.16	361.07	156.69
JUL	554.27	438.41	52.47	0.76	1.74	57.46	111.53	491.63	203.07
AUG	423.33	320.42	49.96	0.99	2.59	44.68	105.17	371.36	170.64
SEP	302.89	220.68	39.31	1.19	3.12	37.55	87.30	261.38	176.12
OCT	101.52	62.52	19.17	1.14	2.08	16.97	92.09	82.94	75.15
NOV	29.88	27.45	1.04	0.51	0.08	1.26	75.08	29.10	69.79
DEC	17.37	10.43	3.19	0.15	0.32	3.30	56.76	13.85	36.81

Table 8. Monthly discharge statics with calibration and validation.

Months	Historical							
	Calibration (2003-2010)				*Validation (2011-2014)*			
	MAX	*AVG*	*MIN*	*STD*	*MAX*	*AVG*	*MIN*	*STD*
JAN	99.89	18.93	0.97	22.13	89.31	16.22	0.06	19.93
FEB	674.70	42.51	0.30	84.42	218.80	60.24	0.00	64.45
MAR	289.60	65.16	1.56	71.14	339.40	70.66	2.77	79.18
APR	415.30	84.19	0.77	92.85	597.70	129.92	4.74	152.30
MAY	797.50	150.47	11.20	167.58	1182.00	275.29	25.10	314.06
JUN	1322.00	260.03	26.83	296.35	1405.00	310.16	30.62	358.12
JUL	1726.00	386.93	45.74	437.88	1719.00	426.63	44.78	462.33
AUG	1356.00	314.99	29.88	351.49	1355.00	316.70	34.55	356.40
SEP	1065.00	256.59	23.30	284.62	979.40	226.17	28.14	258.27
OCT	746.70	154.83	11.55	177.93	468.10	75.39	2.59	97.84
NOV	407.60	79.08	6.78	94.34	331.30	28.33	0.00	69.13
DEC	140.30	30.17	2.70	34.85	96.08	13.95	0.08	21.51

Most Fitted Model

Mainly three model pattern are matching is better than others namely ACCESS-ESM1-5, MPI-ESM1-2-LR and NorESM2-MM. Distance from origin, The sd of the variable being compared is shown by the distance from the origin to a point on the picture. When distances are smaller, it means that the model fits the measured variability better (Fig 7). Angle from the Azimuthal Axis, The association coefficient is shown by the angle between the point that stands for a model and the azimuthal axis. A smaller angle means that the predicted data is more likely to match the actual data, which means that the phase or pattern matching is better. As a result, the model that is closest to the reference point and has a small angle and radial distance is thought to be the best fit to the data shown on the Taylor diagram. To get a full picture of how well a model works, it's important to look at both the radial distance and the azimuthal angle when figuring out what a Taylor diagram means. As you can see, the Taylor diagram shows how well models match up with important statistical features of the real data, like variance and association.

Future Streamflow

The validated model is forced by the bias-corrected data of average scenarios in order to simulate the future impact of climate change on the streamflow of the TRB for future climatic years (2016–2099). This is done in order to forecast the future climate change consequences. When the model was being simulated for future years, the parameters of the model were maintained in the same manner as they were during the verified run. A simulation of future stream flows is also performed using the land-use and cover map that is currently in effect for the current year. The amount of human interference in the research area is extremely low because of the terrain of the area, which is characterised by severe elevations, and the large presence of snow and glaciers. Consequently, during the course of the study, a change in land use that is not notable is taken into consideration. It was just for a single time period that the model was executed, which was from 2016 to 2099. In Table 3, you will see a summary of the monthly discharge statistics for both the current and subsequent months. Additionally, it has been observed that the total yearly discharge of the future from TRB is greater than the climate conditions that are currently in place. It is clear from looking at Figure 4 that the peak streamflow is moving away from the months of May through September and towards the climate future simulations. In addition, the runoff regime of the TRB exhibits an increasing trend across all of the model scenarios. From the data presented in Table 3, it can be deduced that the average annual streamflow from the basin will rise by between 13 and 24 percent in comparison to the current average annual flow.

The precipitation patterns in the region significantly impact the fluctuation of the river flow in the region. In this EHR, the majority of the climate scenarios show a rise in yearly precipitation of approximately 29% and an increase in temperature of approximately 0.21°C to 5.67°C. This leads to an increase in annual flow of approximately 8.75–29.39% towards the end of the century (2099). It is important to note that the estimated hydrological responses are contingent upon the anticipated precipitation and faster melt in the region, both of which are uncertain. The results that were described above make it abundantly evident that the structure is the most significant factor in determining the level of uncertainty that is associated with the simulation of future streamflow under altered climatic circumstances (Table6-9).

Table 9. Monthly discharge statics ACCESS-ESM1-5 (Climate Data).

Months	ACCESS-ESM1-5 (Climate Data)											
	NF (2016-2043)				*MF (2044-2071)*				*FF (2072-209)*			
	MAX	*AVG*	*MIN*	*STD*	*MAX*	*AVG*	*MIN*	*STD*	*MAX*	*AVG*	*MIN*	*STD*
JAN	99.14	29.99	1.27	31.57	109.70	31.82	2.09	34.92	111.90	33.02	1.70	35.61
FEB	78.35	24.42	0.39	26.03	70.98	22.03	0.58	22.91	411.70	77.06	1.09	129.14
MAR	156.00	49.26	1.30	51.03	170.60	53.23	1.27	62.41	172.00	52.46	1.52	57.86
APR	207.30	62.41	1.45	67.50	202.20	60.04	2.29	64.90	233.60	68.05	3.00	80.19
MAY	441.20	121.08	12.81	140.55	654.00	174.96	25.17	205.90	622.60	169.30	24.93	190.17
JUN	975.50	257.65	38.46	304.24	999.40	269.45	36.93	308.89	1119.00	319.29	30.92	361.65

JUL	1612.00	422.37	63.92	500.49	1222.00	318.91	47.23	379.14	1445.00	374.65	67.15	442.45
AUG	1243.00	328.57	50.88	387.07	1240.00	335.21	39.36	383.63	1278.00	321.93	66.54	393.48
SEP	1015.00	272.82	37.48	315.24	845.80	223.72	29.89	261.20	903.80	244.23	27.66	276.79
OCT	547.80	148.17	17.46	172.55	453.40	119.02	17.56	141.24	509.60	135.07	18.09	156.15
NOV	327.20	93.32	8.84	101.92	208.70	54.29	6.90	66.38	406.20	119.36	9.06	125.56
DEC	119.00	32.13	3.76	37.67	180.00	50.80	3.93	60.84	105.70	28.26	3.79	31.97

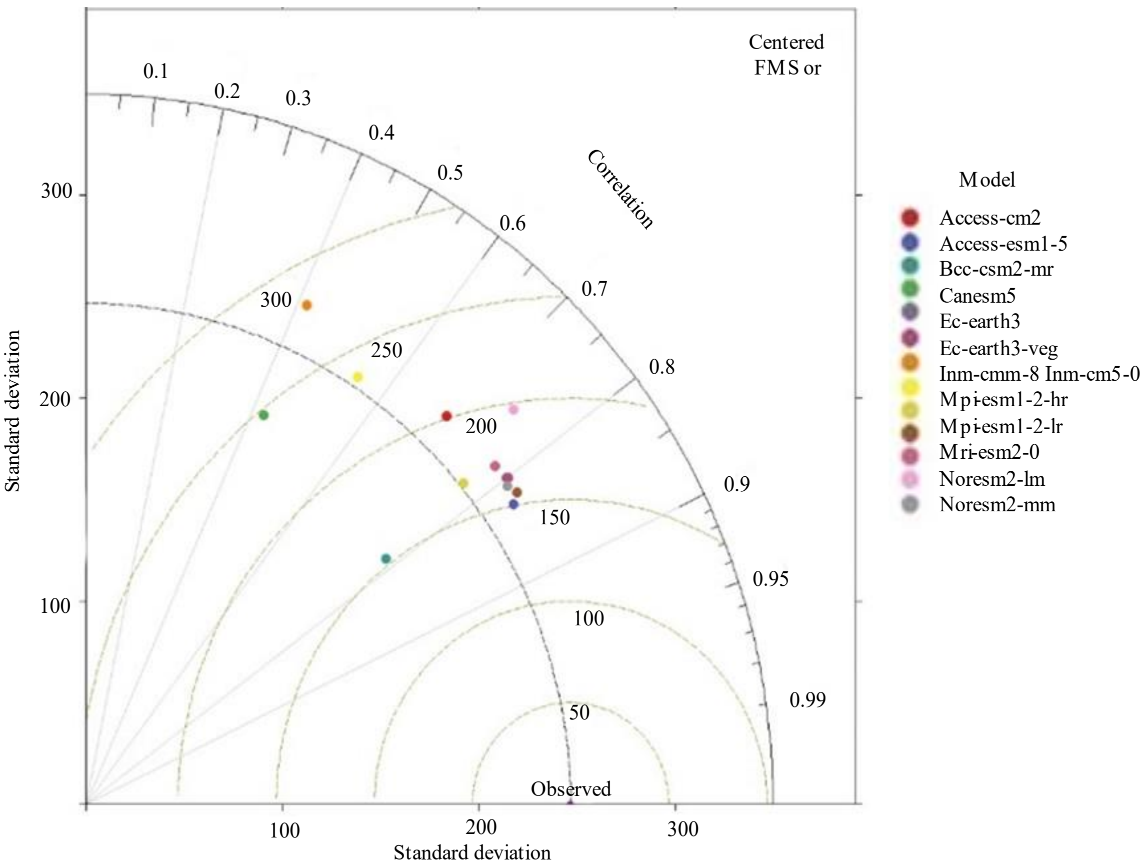

Figure 7. Most fitted value of all 13 models.

CONCLUSION

The modeling of the hydrological behavior of snow- and rain-fed river basins in the Himalayas is extremely important since a significant population depends on the water found in the Himalayan rivers in various ways. This study analyzes the potential impact climate change could have on streamflow by utilizing three climates that are projected to occur in the 21st century. When applied to the TRB at the Teesta IV DAM gauging station, the SWAT model is utilised in an effective manner. The calibration, validation, and uncertainty analysis were all performed with the assistance of a sophisticated SUFI-2 algorithm. The SWAT model was found to have a satisfactory performance during both the calibration and validation periods, according to the results of the SWAT modeling and the evaluation criteria. Based on the findings, it can be observed that the simulation uncertainty range is within a reasonable range (R factor < 1), which encompassed the observations the majority of the time (P factor > 50%). Over the course of both time periods, the values of R2 and NSE are found to be greater than 0.87 and 0.89, respectively. It demonstrated a high level of efficiency in the model as well as a good connection between the discharge that was measured and the discharge that was predicted. Despite the fact that not all of the peaks and the flow of the lean time could be replicated accurately, the contour of the hydrograph has been regenerated in a satisfactory manner overall. In the basin, the water output accounts for around sixty percent of the precipitation. In terms of the water yield, the contribution from snow and glacier melt amounts to around 74% of the total. The ET accounts for about 29% of the basin's total precipitation. During the flood forecasting and streamflow simulation of the TRB, it is imperative that these aspects be taken into consideration. To this purpose, the SWAT model can be considered to be an ideal instrument for simulating the streamflow and the various components of the water balance for a Himalayan basin and its surrounding environment.

The findings of this research, taken as a whole, provide valuable insights that can be utilized to enhance the management of water resources and modeling practices, particularly with regard to the challenges that are given by uncertainty. By establishing the framework for assessments that are both more accurate and trustworthy when carried out in the field, this study provides a substantial contribution to the advancement of water resource modeling and establishes the foundation for more accurate and trustworthy evaluations. In this research, the applied model and a programming language. First, use QSWAT for simulation. It is a source application that provides help, which is an easy task but requires more refinement requirements because QSWAT uses the TAUDEM program based on Python. After that, use machine learning/programming language R, i.e., provide help for data arrangement as per SWAT model, Taylor diagram for the best-fitted model, and lastly, shiny RSWAT model. SWATCUP is a very efficient and time-saving program and also helps with multiple objective functions in a single time, but refinement is required to give simple solutions.

REFERENCES

1. Aayog, N. I. T. I. (2018). Sustainable Tourism in the Indian Himalayan Region. *Report of Working Group II, NITI Aayog, Government of India*.
2. Abbas, T., Hussain, F., Nabi, G., Boota, M. W., & Wu, R. S. (2019). Uncertainty evaluation of SWAT model for snowmelt runoff in a Himalayan watershed. *Terrestrial, Atmospheric & Oceanic Sciences*, *30*(2).
3. Abdul Hakeem, K., Abirami, S., Rao, V. V., Diwakar, P. G., &Dadhwal, V. K. (2018). Updated inventory of Glacial Lakes in Teesta Basin using remote sensing data for use in GLOF risk assessment. *Journal of the Indian Society of Remote Sensing*, *46*, 463-470.
4. Amoako Johnson, F., & Hutton, C. W. (2014). Dependence on agriculture and ecosystem services for livelihood in Northeast India and Bhutan: vulnerability to climate change in the Tropical River Basins of the Upper Brahmaputra. Climatic change, 127, 107-121.
5. Basnett, S., Kulkarni, A. V., & Bolch, T. (2013). The influence of debris cover and glacial lakes on the recession of glaciers in Sikkim Himalaya, India. *Journal of Glaciology*, *59*(218), 1035-1046.
6. Berthier, E., Arnaud, Y., Kumar, R., Ahmad, S., Wagnon, P., & Chevallier, P. (2007). Remote sensing estimates of glacier mass balances in the Himachal Pradesh (Western Himalaya, India). *Remote Sensing of Environment*, *108*(3), 327-338.
7. Covey, C., AchutaRao, K. M., Fiorino, M., Gleckler, P. J., Taylor, K. E., & Wehner, M. F. (2002). Intercomparison of climate data sets as a measure of observational uncertainty. *PCMDI Report*, *69*.
8. Das, S., Datta, P., Sharma, D., & Goswami, K. (2022). Trends in temperature, precipitation, potential evapotranspiration, and water availability across the teesta river basin under 1.5 and 2 C temperature rise scenarios of CMIP6. *Atmosphere*, *13*(6), 941.
9. Du, X., Silwal, G., & Faramarzi, M. (2022). Investigating the impacts of glacier melt on stream temperature in a cold-region watershed: Coupling a glacier melt model with a hydrological model. *Journal of Hydrology*, *605*, 127303.
10. Gleckler, P. J., Taylor, K. E., &Doutriaux, C. (2008). Performance metrics for climate models. *Journal of Geophysical Research: Atmospheres*, *113*(D6).
11. Goyal, M. K., Shivam, Sarma, A. K., & Singh, D. S. (2018). Subansiri: largest tributary of Brahmaputra River, Northeast India. *The Indian Rivers: Scientific and Socio-economic Aspects*, 523-535.
12. Grusson, Y., Sun, X., Gascoin, S., Sauvage, S., Raghavan, S., Anctil, F., &Sáchez-Pérez, J. M. (2015). Assessing the capability of the SWAT model to simulate snow, snow melt and streamflow dynamics over an alpine watershed. *Journal of Hydrology*, *531*, 574-588.

13. Guo, J., & Su, X. (2019). Parameter sensitivity analysis of SWAT model for streamflow simulation with multisource precipitation datasets. *Hydrology Research*, *50*(3), 861-877.
14. Huang, X., Sillanpää, M., Gjessing, E. T., Peräniemi, S., & Vogt, R. D. (2011). Water quality in the southern Tibetan Plateau: chemical evaluation of the YarlungTsangpo (Brahmaputra). *River research and applications*, *27*(1), 113-121.
15. Kaser, G., Großhauser, M., &Marzeion, B. (2010). Contribution potential of glaciers to water availability in different climate regimes. *Proceedings of the National Academy of Sciences*, *107*(47), 20223-20227.
16. Khawas, V. (2015). Pathways for Climate Resilient Livelihoods: The Case of a Large Cardamom Farming in the Dzongu Valley of the Tista River Basin, Sikkim Himalaya. *Climate Change in the Asia-Pacific Region*, 319-334.
17. Kouchi, D. H., Esmaili, K., Faridhosseini, A., Sanaeinejad, S. H., Khalili, D., & Abbaspour, K. C. (2017). Sensitivity of calibrated parameters and water resource estimates on different objective functions and optimization algorithms. *Water*, *9*(6), 384.
18. Kumar, B., Lakshmi, V., Patra, K. C., Sen, I. S., & Srinivasan, R. (2016, December). Assessing Hydrological Uncertainties Using the SWAT Model to Simulate Streamflow Over the Alpine Himalayas. In *2016 AGU Fall Meeting*. AGU.
19. Mishra, V., Bhatia, U., & Tiwari, A. D. (2020). Bias-corrected climate projections for South Asia from coupled model intercomparison project-6. Scientific data, 7(1), 338.
20. Mukhopadhyay, S. C. (1982). *The Tista basin: a study in fluvial geomorphology*. KP Bagchi.
21. Nguyen, T. V., Dietrich, J., Dang, T. D., Tran, D. A., Van Doan, B., Sarrazin, F. J., ... & Srinivasan, R. (2022). An interactive graphical interface tool for parameter calibration, sensitivity analysis, uncertainty analysis, and visualization for the Soil and Water Assessment Tool. *Environmental Modelling & Software*, *156*, 105497.
22. Rahman, K., Maringanti, C., Beniston, M., Widmer, F., Abbaspour, K., & Lehmann, A. (2013). Streamflow modeling in a highly managed mountainous glacier watershed using SWAT: the Upper Rhone River watershed case in Switzerland. *Water resources management*, *27*, 323-339.
23. Raj, K. B. G., Remya, S. N., & Kumar, K. V. (2013). Remote sensing-based hazard assessment of glacial lakes in Sikkim Himalaya. *Current Science*, 359-364.
24. Raman, A., Kulkarni, A. V., & Prasad, V. (2022). Glacier mass balance estimation in Garhwal Himalaya using improved accumulation area ratio method. *Environmental monitoring and assessment*, *194*(8), 583.
25. Rupper, S., Johnson, E., Olson, M., Steenburgh, J., Kochanski, A., Riley, C., & Skiles, M. (2020, July). Climate-Driven Glacier and Snowpack Changes in the Water Towers of Asia (Invited Presentation). In *19th Conference on Mountain Meteorology*. AMS.
26. Sam Albers, Ilaria Prosdocimi (2023). Link: https://github.com/cran-task-views/Hydrology/
27. Sharma, A., & Goyal, M. K. (2020). Assessment of the changes in precipitation and temperature in Teesta River basin in Indian Himalayan Region under climate change. *Atmospheric Research*, *231*, 104670.
28. Shukla, A. K., Ahmad, I., Jain, S. K., & Verma, M. K. (2024). Assessment of Continuous Growth of Glacial Lakes in the Teesta River Basin Using Semi-Automated Geospatial Approach. *Nature Environment & Pollution Technology*, 23 (2), 875-886. https://doi.org/10.46488/NEPT.2024.v23i02.023.
29. Shukla, A. K., Ahmad, I., Jain, S. K., & Verma, M. K. (2024). Enhancing Model Calibration and Uncertainty Estimation through MultiObjective Optimization with SUFI-2 Algorithm. *Journal of Environmental Informatics Letters*, 11(2) 109-122. https:// doi:10.3808/jeil.202400130.
30. Shukla, S., Jain, S. K., & Kansal, M. L. (2021). Hydrological modelling of a snow/glacier-fed western Himalayan basin to simulate the current and future streamflows under changing climate scenarios. *Science of the Total Environment*, *795*, 148871.
31. Singh, V., Kumar Goyal, M., Surampalli, R. Y., & Munoz-Arriola, F. (2017). Sub catchment assessment of snowpack and snowmelt change by analyzing elevation bands and parameter sensitivity in the high Himalayas. *Hydrology and Earth System Sciences Discussions*, 1-31.

32. Schürz, C. (2019). Development of tools and interfaces for the implementation, pre-processing, and sensitivity analysis of the SWAT model in an R programming environment.
33. Talukdar, S., Eibek, K. U., Akhter, S., Ziaul, S. K., Islam, A. R. M. T., & Mallick, J. (2021). Modeling fragmentation probability of land-use and land-cover using the bagging, random forest and random subspace in the Teesta River Basin, Bangladesh. *Ecological indicators*, *126*, 107612.T
34. sering, T., Wahed, M. S. A., Iftekhar, S., & Sillanpää, M. (2019). Major ion chemistry of the Teesta River in Sikkim Himalaya, India: Chemical weathering and assessment of water quality. *Journal of Hydrology: Regional Studies*, *24*, 100612.
35. Wu, Y., & Liu, S. (2012). Automating calibration, sensitivity and uncertainty analysis of complex models using the R package Flexible Modeling Environment (FME): SWAT as an example. *Environmental Modelling & Software*, *31*, 99-109.
36. Zaman, S., &Pramanick, P. (2020). Ecosystem Services of Mahananda Wild Life Sanctuary: An Overview of Faunal and Floral Diversity. NATURAL RESOURCES AND THEIR ECOSYSTEM SERVICES, 63.
37. Zannah, R., Mohammed, K., Rahman, A., & Yunus, A. (2020). Analysis on flow and water balance parameters of Teesta River basin due to climate change and upstream intervention. In *Water, Flood Management and Water Security Under a Changing Climate: Proceedings from the 7th International Conference on Water and Flood Management* (pp. 267-282). Springer International Publishing.
38. Zhang, Y., Luo, Y., Sun, L., Liu, S., Chen, X., & Wang, X. (2016). Using glacier area ratio to quantify effects of melt water on runoff. *Journal of Hydrology*, *538*, 269-277.

